 https://doi.org/10.3311/PPci.19987

Periodica Polytechnica Transportation Engineering, 66(4), pp. 1032–1047, 2022

Combining Discrete Wavelet Transform and Strong Ground Motion Duration to Reduce Computational Costs in Dynamic Analysis of Structures

Behrooz Shahriari[1*], Noorollah Majidi[2]

[1] Faculty of Mechanics, Malek Ashtar University of Technology, 84145-115 Isfahan, Iran
[2] Department of Civil Engineering, University of Isfahan, 8174673441 Isfahan, Iran
[*] Corresponding author, e-mail: shahriari@mut-es.ac.ir

Received: 08 February 2022, Accepted: 21 June 2022, Published online: 05 July 2022

Abstract

The dynamic time history analysis is the most accurate method for calculating the structure response relative to the vibrating load. The use of this method is time-consuming due to the long-duration earthquakes and is generally less commonly used. Wavelet transforms are one of the new methods for filtering waves. The duration of a strong ground motion is actually a concept that can be used to turn an earthquake with a long time into an earthquake with a shorter time. In this paper, two concepts of filtration using wavelet transform and the use of a duration of strong ground motion are used for the time history analysis of structures. For this purpose, the acceleration of the earthquake in 5 states was filtered by wavelet transform. In each stage, the high and low frequencies are separated, and the number of earthquake acceleration points is half-past. Then the beginning and the end of the main earthquake and the approximate waves obtained from the wavelet transform are removed using the concept of the duration of the strong ground motion. Finally, two two-dimensional and three-dimensional structures are analyzed using the main earthquake and the waves obtained by combining the two concepts of wavelet transform and the duration of strong ground motion. The results show that by reducing the number of acceleration points of the main earthquake record to more than 95%, the dynamic response error is less than 8%.

Keywords

time history analysis, wavelet theory, duration of the strong ground motion, structural dynamic analysis

1 Introduction

With the expansion of cities and the increase in population and the need for high-density buildings, engineers have to move more and more to recognize the earthquake as a destructive, accidental, and indeterminate force. The earthquake is an influential force in the design of structures. One of the important parameters in determining the earthquake specification is its frequency content [1, 2]. The serious approach of researchers and practitioners in accepting this phenomenon, not in its devastating way, but in recognizing as much as its related sciences have led to the preparation and compilation of books, essays, and articles throughout the world [3]. Earth movements are recorded by accelerometers and seismographs. Seismographs are very sensitive devices that can record earthquake-induced earthquake events. Data from seismic devices cannot be used directly in earthquake engineering, since they are not able to record strong earth movements at distances close to earthquake centers [4]. Unlike seismographs, accelerometers are very suitable for installation near active earthquake centers and active faults and in important structures, and they can record acceleration that is important in earthquake engineering [5].

By examining the records recorded in various earthquakes, it is observed that the use of the total duration of the earthquake is time-consuming. For this reason, the use of a part of the earthquake with its predominant energy has been found among researchers. The total duration of an earthquake depends on factors such as earthquake magnitude. Several methods have been proposed to calculate the important duration of acceleration. In reference [6], the enclosed time period, in which the time interval between the first and the last amplitude of acceleration is greater than a certain value (usually 0.05 g), was considered as a time of strong motion. Trifunac and Brady [7, 8] defined the period of strong vibration as a time interval in which the square integral of the accelerations is a way

Cite this article as: Shahriari, B., Majidi, N. "Combining Discrete Wavelet Transform and Strong Ground Motion Duration to Reduce Computational Costs in Dynamic Analysis of Structures", Periodica Polytechnica Civil Engineering, 66(4), pp. 1032–1047, 2022. https://doi.org/10.3311/PPci.19987

of achieving strong ground motion. They chose the time interval between 5% and 95% as a strong motion.

There are different methods for determining the duration of a strong earthquake, and in this article, two of them, namely uniform and significant duration, have been studied. In most seismological studies for investigating earthquake acceleration, its significant time is investigated. Research shows that the effect of strong ground motion duration plays an important role in distributing energy to the structure and causing damage [7, 8].

The dynamic response of structures is determined for the strong ground motion using one of the methods for analyzing the spectrum of response or time history analysis. Generally, for the seismic analysis of important structures such as power plants, dams, tall structures, suspended bridges, and the study of the vulnerability of structures, it is necessary to analyze the time history. On the other hand, dynamic analysis in these structures is time consuming, so in this type of structure, it is necessary to use methods to reduce computational costs.

In this paper, in addition to the concept of strong earthquake duration, wavelet transforms (WT) have also been used to reduce the duration of the dynamic analysis. In this method, in each step, the number of accelerated earthquake mapping points was reduced to half of the previous points, so that in the first step of fifth, the number of main earthquake points was 32 times lower.

The WT has been around for about three decades [9]. The history of the use of wavelet theory for dynamic analysis of structures dates back to about 18 years ago [10]. From a mathematical point of view, the transform provides more information about the crude wave. An earthquake wave is an unstable wave because its frequencies do not occur during the entire time of the wave, and at different moments have different frequencies. In the reference [10], the dynamic response of the structures was calculated using discrete wavelet transforms (DWT) that were combined with the fast Fourier transform method. The results showed that the required time in this method was half the time in the common analysis, and its error was less than 2%.

One of the best methods for analyzing the earthquake wave is the use of WT. The WT is divided into two groups: continuous and discrete. Given the nature of the earthquake acceleration, DWT is more appropriate [11].

In [12], structures were optimized using an wavelet network. To optimize the modified genetic method, which was combined with simulated annealing (SA), was used to reduce the dynamic computations. For this purpose, after separating the high and low frequencies of the earthquake, the number of accelerated earthquake points was reduced, then the wavelet function was used as the stimulation function in the neural network. The analysis time in this method was about 10% of the time used by the neural network, while its error was less than 8%.

Heidari and Majidi [13] using discrete wavelet theory, reduced the calculations in the earthquake displacement curve and earthquake speed curve by more than 93 percent. They showed that by using the Haar wavelet function, the calculations could be reduced by an error of less than 5%.

Majidi and Heidari [14] in another study, could investigate the relationship between earthquake frequencies and the natural frequency of structures using discrete wavelet theory. In this study, they used a wavelet transform method as an alternative to modal analysis.

In [15], the dynamic analysis of the structure was performed using a wavelet neural network, in this paper, the error was negligible, while the analysis time was reduced by 90%.

In [16], the dynamic response of the structure for five stages was estimated using wavelet transformation. The results showed that with increasing each stage, the time of the analysis was halved, and the error was doubled.

In [17] wavelet theory and genetic methods were used for earthquake optimization analysis. The error rate was about 2%, and the time needed to optimize was 15% of the time when the wavelet was not used.

Furthermore, using earthquake acceleration analysis and using dynamic analysis, the structures were optimized by a genetic method. The results clearly showed the ability of the method to reduce the optimization time [18].

In [19], the non-linear response spectrum of the structures was calculated using the wavelet transforms. Results showed that the error in using the wavelet transforms, in this case, was less than 10%.

The cost of calculations is more important in elasto-plastic analysis than in elastic analysis [20, 21]. Because generally, with the nonlinearity of the structure, the cost of calculations also increases. In this regard, Kamgar et al. [22] examined the performance of WT in a 7-story, two-dimensional structure. The results of this paper showed the optimal performance of wavelet transform in this category of problems.

In a study, Kamgar et al. [23] examined the performance of WT in the analysis of linear single-degree-freedom-systems. In this study, the record of earthquakes of

far-fault and near-fault was evaluated. The results of this paper showed that using the approximate wave of the third level has the error of less than 10%.

One of the challenges of incremental dynamic analysis (IDA) is the high cost of computing. Using wavelet transform to reduce the cost of computing can also be helpful in this area. Dadkhah et al. [24] examined the performance of using WT for IDA in a 6-story, 2D structure. In this study, 15 earthquake records were investigated. Examination of the displacement response, drift, and base shear showed that the calculation error for the approximate wave obtained from the third stage is always less than 10%.

Other time-consuming dynamic problems are those dynamic analyzes that consider the effects of soil-structure interaction. Kamgar et al. [25] in a study investigated the performance of wavelet transform in soil-structure interaction problems. In this study, by examining the structures of 20, 25, 30, and 35 story, they showed that the last reliable approximate wave is related to the third level of wavelet transform.

Javadanian et al. [26] examined the use of the wavelet method to obtain site responses. In this study, only the single-degree response of freedom systems was examined. The results presented in this paper also showed the proper performance of the approximate third wave obtained from the wavelet transform.

Analysis of peridynamic models is another time-consuming dynamic issue. In this regard, Majidi et al. [27] examined the performance of WT in reducing the cost of calculations in such problems. The Sarpol-e Zahab earthquake was also studied in this study. The results of this study showed that the dynamic response of the structure and the shape of the crack in the studied concrete beams had a suitable accuracy for the approximate wave of the third and fourth levels.

Previously, the use of strong ground motion duration and wavelet transform separately has been proposed in various studies and for different problems in order to reduce the cost of calculations. This means that one group of studies reduces the loading time to reduce the cost of dynamic analysis calculations of structures under earthquake vibration, and another group modifies the earthquake time step (down-sampling methods). In this study, the use of these two methods simultaneously to reduce the cost of calculations in the dynamic analysis is investigated. In fact, in this study, both the duration of the earthquake record is reduced, and the time step of the earthquake record is modified. The method proposed in this paper is used in all dynamic problems such as incremental dynamic analysis, dynamic analysis considering soil-structure interaction, and all linear and nonlinear dynamic analyses.

It can be said that if the critical time step of the numerical method used for dynamic analysis is not problematic in the analysis process, this method has good accuracy to reduce the cost of calculations in dynamic analysis. This fact has been well demonstrated in studies on the use of wavelet transform for dynamic analysis. In fact, all studies have shown that the use of wavelet transform can be useful in a variety of dynamic problems.

In this paper, for the first time, the duration of strong ground motion and wavelet transformation has been used to reduce the time of dynamic computing. For this purpose, first, the acceleration of the earthquake is filtered by way of band-pass and down-sampling, so that its noise can be eliminated, and the high and low frequencies are separated. Thus, two waves, one containing high frequencies, and the other containing low frequencies, are obtained, with the number of points of each of these two waves being half the number of points of the main wave. Then this separation of frequencies is repeated on a wave containing low frequencies. In each stage, the number of new wave points is half the number of wave points in the previous stage. Since, according to previous studies, clearly that the approximate wave is more similar to the original wave [15, 23, 25, 28, 29], therefore, this wave section is used for dynamic analysis. At each stage of the frequency separation, the maximum acceleration of the approximate wave equates to the maximum acceleration of the original earthquake. This is done by multiplying all the approximate wave points in the maximum acceleration of the original earthquake and dividing it by the maximum acceleration of the approximate magnitude. In the next step, the number of earthquake points is reduced by using a significant and uniform time. In fact, with wavelet transform, the time step of the analysis becomes larger, and with the duration of the strong ground motion, the duration of the analysis decreases. Then, using the wave that once filtered using the wavelet theory and then reduced with a significant and uniform time, and finally, two structures are analyzed.

2 Wavelet transform

In the WT, there are different mother and scale functions [30–32]. Mother functions (ψ) and wavelet scales (φ) are shown and shown, some of the mother functions have an explicit mathematical relation, and some of them do not

have explicit mathematical expressions. In this research, the Haar wavelet function was used, which is shown in Fig. 1 of the mother function and its scale.

In the WT, there are two parameters of scale and transition. The scale, like a mathematical function, compresses or expands a wave. The large scale corresponding to the opening of the wave and the small scales cause the wave to compress. In a wavelet, the scale has a photo-frequency relationship. The low frequency (large scale) corresponds to the general information of the wave and the large frequency, corresponding to the wave details. The high frequencies for a long time are unscathed by the wave, while there are low frequencies throughout the wave. In the continuous wavelet transform, the transmission parameters and the scale change continuously. In fact, the rate of change in the computer at each stage is very small (continuous). This increases computer computing [33]. In the case of wavelet transformation, transmission, and scale being considered discrete, another type of wavelet transformation is called the DWT [34]. In high scales (low frequencies), the sampling rate of time curve points can be reduced in accordance with the Nyquist norm and reduce the volume of computations. Nyquist sampling is the minimum permissible sampling rate of the continuous wave that can be reconstructed [35].

For an S wave with several N points, it is possible to remove high frequencies using downstream filters and obtained approximately the main wave. Using the high-pass filter, you can also remove the lower frequencies and obtain the waveform details. With the simultaneous effect of these two filters on the wave, it can be divided into two parts with high and low frequencies. Approaches and wave details are shown and displayed at each stage. But the problem is that at each stage, using filters, the main wave is obtained from the main wave with the number of points equal to the main wave, which doubles the number of wave points. To overcome this problem, the down-sampling sample reduction basis is used [35]. Considering that the maximum wave energy is approximate, and the shape of this part of the wave is more similar to the wave, the filtering operation on this part of the wave is done and the wave

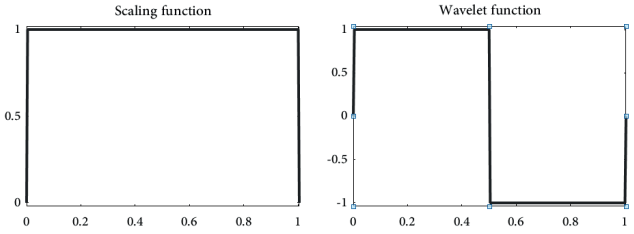

Fig. 1 Mother and scale wavlet (Haar)

A1 is converted into two waves A2 and D2 [35]. The number of points each of these waves is approximately half the number of points A (one-fourth of fourth of the original wave S). Although, from a theoretical point of view, this can be done log2N on a number of occasions, but it is needed in dynamic wave analyzes that are more similar to the original wave, and the number of points is sufficiently small. In fact, the rapid conversion of the wavelet acts like a filter bank [36]. There are several methods in this regard. In this research, the Mallat method [35], used in dynamic work [15], has been used. In this method, the approximate waves Aj and partial Dj are obtained from the initial wave S using the following relationships [36].

$$A_j = ap_{j,k} = \sum_n s(n) h_j^*(n - 2^j k) \tag{1}$$

$$D_j = de_{j,k} = \sum_n s(n) g_j^*(n - 2^j k) \tag{2}$$

Where h_j is the downstream filter (mother function), and g_j is the high-pass filter (scale function). The values of h and g are obtained from one step to the next using the following relationships [37].

$$g_1(n) = g(n) \tag{3}$$

$$h_1(n) = h(n) \tag{4}$$

$$g_{j+1}(n) = \sum_k g_j(k) g(n - 2k) \tag{5}$$

$$h_{j+1}(n) = \sum_k h_j(k) g(n - 2k) \tag{6}$$

These relationships indicate that this method is similar to the theory of filters and that the rapid the WT is the same as the filtering of the filter bank. The inverse of it is also the same as the combination of the filter bank. The filters that are used in the wavelet reverse conversion are shown and represented by the following relationships.

$$\tilde{h}_j(n - 2^j k) = 2^{-0.5j} \tilde{\psi}(2^{-j}(t - 2^j k)) \tag{7}$$

$$\tilde{g}_j(n - 2^j k) = 2^{-0.5j} \tilde{\varphi}(2^{-j}(t - 2^j k)) \tag{8}$$

The values (ψ) and (φ) functions of the mother and the function of the scale. By having the values and the main wave, it can be reconstructed using the following relationship. In Fig. 2, the down-sampling method is shown in two stages, where N is the number of initial curve points. Furthermore, A and D are respectively the wave of approximate and detailed information.

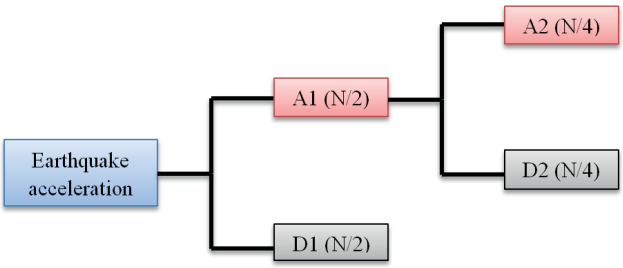

Fig. 2 WT with down-sampling algorithm up to two stages of filtering

3 Time of strong ground motion

The duration of the earthquake is one of the seismic parameters that refer to the total time during which the earthquake occurred. The initial studies on the time of a strong ground motion show the dependence of this parameter on the magnitude of the earthquake and the focal length [38]. The duration of a strong ground motion is a parameter that at that time, there is dominant earthquake energy to vibrate a structure. This parameter is also important in nonlinear analyzes. The first definition for this parameter is called the bracketed time period, which is the time between the first and last time the acceleration of the earth is greater than 0.05 g [8, 39]. Brady and Trfunac have a relationship that can be obtained by having any of the acceleration, velocity, or displacement functions, for the duration of a strong ground motion [8]. The duration of strong ground motion for the production of artificial acceleration also used [8, 40]. To provide the relationship between the times of the strong ground motion, we must use parameters that depend on the duration and intensity of the average energy. According to Housner [41], the time of strong propulsion is strongly dependent on Arias. Considering the total time of earthquake causes a significant increase in dynamic analysis time. Therefore, in some cases, due to the small effect of the initial and end parts of the earthquake acceleration on the dynamic behavior of structures, these parts can be removed, and seismic loading can be done in a shorter time. It should be noted that the new shortened wave must have a large volume of seismic energy. Considering the above, there are 4 methods for determining the duration of strong ground motion which are uniform, bracketed, effective, and significant [42]. The total amount of time between the Arias intensity, which is usually between 5 and 95% of the Arias intensity, is a significant time. In this method, Arias intensity is expressed in terms of percentage and time in seconds. An effective period is usually 90% of the total earthquake energy and is the duration of an earthquake where more than 90% of earthquake energy exists. This time is in the range of 5 to 95% of the Arias intensity of the earthquake. The uniform duration is the sum of the times when the acceleration is greater than a certain value; usually, this value is 5% of the maximum earthquake acceleration. The time period between the first and last time the acceleration of the earth's motion exceeds a certain amount of time is called a selective time. Usually, the maximum acceleration value is 5% [42, 43]. Based on the said concepts, the steps of this research are defined as follows:

1. Correction of the earthquake using the band-pass method (presumably, if the record does not need to be corrected, this step is eliminated).
2. Modified earthquakes in the previous stage are divided into approximate and detail waves by using Haar wavelet in five steps.
3. At each stage, the approximate waves are scaled based on the maximum acceleration of the main earthquake.
4. A uniform, significant, and bracketed duration for the main wave of the earthquake and each of the approximate waves is calculated.
5. A part of the approximate waves that have been uniform, significant, and bracketed during a period of time are separated and considered as new accelerations.
6. Several structures are analyzed against these new acceleration waves, and their dynamic response is calculated and compared with each other.

The process is said to have done many earthquakes. In this paper, the results of this analysis method are described for two and three-dimensional structures under the Sarpol-e Zahab earthquake in Iran.

4 Sarpol-e Zahab earthquake

In the November 12, 2017, time international 18: 18: 16, a powerful earthquake with magnitude 7.3 on the Richter scale Iran-Iraq border region in the province around the city Sarpol-e Zahab struck. The reason for choosing this earthquake was that in previous studies, this earthquake has been used to solve various dynamic problems using wavelet [13, 27, 44-46]. In this paper, the L component for this earthquake is investigated. For this purpose, the recorded record has first been modified using the bandpass method with a frequency range of 0 to 30 Hz recorded. The maximum acceleration in the unmodified record is 684.42 and in the modified record is 681.45 cm/s^2. In Fig. 3, the accelerated curve of the modified component of this component is shown. The maximum modified acceleration of the L components is 0.43% with the initially recorded value. The time step of this earthquake is 0.005 and the number of points of this earthquake wave is 19890. The total duration of the earthquake is 99.45 seconds.

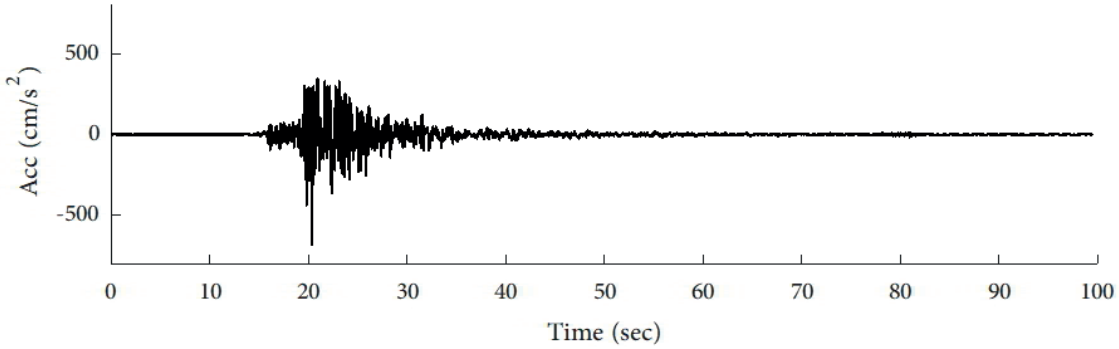

Fig. 3 Modified acceleration of a seismic earthquake

Fig. 4 shows the Arias intensity curve for the main earthquake and the approximate waves. As can be seen in the figure below, the error for wave A5 is too large.

Arias intensity is a concept to represent wave energy. As can be seen, the energy of the approximate wave A5 is very different from other approximate waves. In other words, the energy of the approximate waves A1 to A4 is very close to the main wave of the earthquake, but this is not the case with A5. It can be said that the main reason for this error for the A5 wave is the omission of the main frequency of the earthquake wave in the fifth level of decomposition. In other words, in the wavelet transform at each level of wave decomposition, half of the high frequencies are removed. This means that if the main wave of the earthquake contains frequencies from 0 to 100 Hz. Frequencies of 50 to 100 Hz are removed to make the approximate wave of the first stage (A1). Frequencies of 25 to 50 Hz are also removed to make the approximate wave of the second stage (A2). Thus, the removal of high-frequency frequencies can lead to the elimination of the dominant frequencies of the earthquake record. Therefore, it is predicted that the approximate wave error of A5 in the dynamic analysis is high. In the following, the approximate waves and the main wave of the earthquake are compared in the domain of time and frequency. As shown in Fig. 5, the error of the A5 wave is high in both the time domain and the frequency domain. Therefore, it can be predicted that the calculation error of this wave in dynamic analysis of structures of single degree of freedom and multi degrees of freedom can be high.

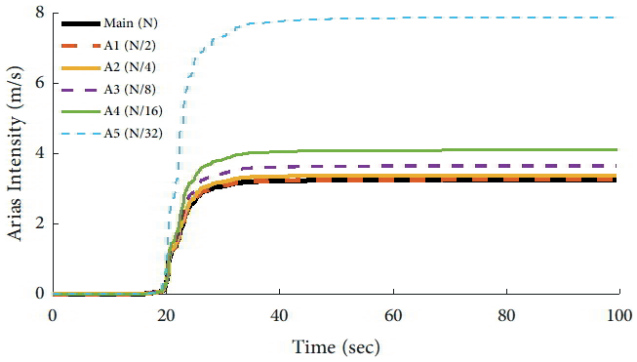

Fig. 4 Arias intensity for main earthquakes and approximate waves

Fig. 6 show the spectral acceleration curve for the main earthquake and the approximate waves. As can be seen in the figure below, the error for wave A5 is too large.

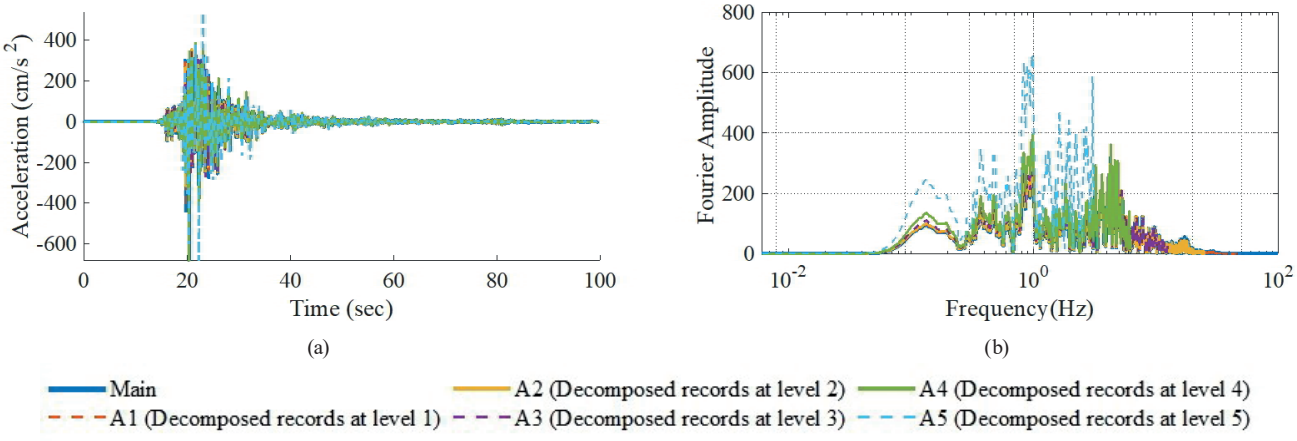

Fig. 5 Main wave and approximate waves obtained from wavelet transform in; a) time domain, b) frequency domain

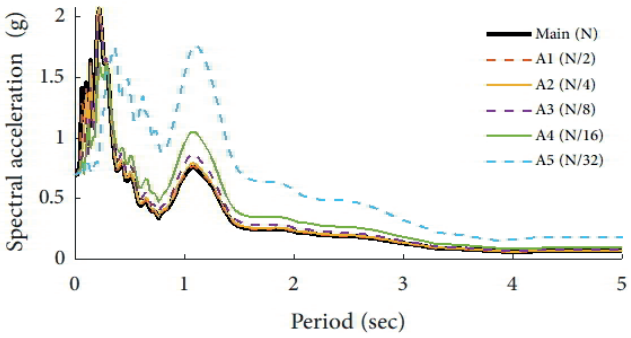

Fig. 6 Spectral acceleration for main earthquakes and approximate waves

4.1 The significant and effective time of the earthquake

For this record, the significant and effective time is obtained identically and therefore, synchronously shown in a single table. Table 1 shows the number of points in each record, the significant and effective time of the earthquake, its start time, and the time it ended, as well as the percentage error of estimating them as compared to the value obtained from the main earthquake.

As shown in Table 1, the significant and effective time of the main earthquake and the approximate wave, A1 to A5 are 10.835, 10.98, 11.02, 11.12, 11.52, and 12.16 seconds, respectively. The error of using the waves A1 to A4 to determine the time is less than 7%. The starting time in the curves of the significant time range from A1 to A4 is almost the same. For an A4 wave, the start error is about 0.5%. The end-time error for the A4 wave is about 3%. Based on the obtained results, instead of using the original earthquake with 19890 points, an A4 curve with 1244 points can be used, whose number of points is 0.0625 the number of major earthquake points, based on this, it can be said that the volume of calculations is significantly reduced.

4.2 The uniform time of the earthquake

Table 2 shows the uniform time, the start time and end time, as well as the estimated errors, relative to the value of the main earthquake.

As shown in Table 2, the time constant for the main earthquake and the A1 to A5 waves is 24.65, 26.38, 26.4, 26.4, 26.00, and 27.84 seconds, respectively. The error of using the waves A1 to A4 to determine the uniform duration is less than 5%. The starting time for the uniform time curves from A1 to A4 is approximately the same. For an A4 wave, the start error is about 0.2%. The end time is uniformly curved curves is almost the same in waves A1 through A4, and the error for the A4 wave is about 4%. Based on the results obtained, instead of using the main earthquake, the A4 curve can be used to reduce the volume of calculations.

4.3 The bracketed time of the earthquake

In Table 3, the values of the bracketed time start and end time, as well as their estimation error, are shown about the value obtained from the main earthquake.

Table 2 Uniform time for main earthquakes and approximate waves

Record name	Uniform duration (sec)	Time (sec)		Percentage difference in time estimate (%)	
		Start	End	Start	End
Main	24.65	15.89	40.54	-	-
A1	26.38	15.89	42.27	0.00	4.267
A2	26.40	15.88	42.28	0.006	4.292
A3	26.40	15.88	42.28	0.006	4.292
A4	26.00	16.24	42.24	0.218	4.193
A5	27.84	15.52	47.36	0.231	16.822

Table 3 Bracketed time for main earthquakes and approximate waves

Record name	Earthquake duration (sec)	Time (sec)		Percentage difference in time estimate	
		Start	End	Start	End
Main	24.65	15.89	40.54	-	-
A1	26.39	15.89	42.28	0.00	4.513
A2	24.42	15.88	42.30	0.062	4.563
A3	26.44	15.88	42.32	0.062	4.612
A4	26.08	16.24	42.32	2.202	4.612
A5	32.00	15.52	47.52	2.328	17.466

Table 1 Significant time for main earthquakes and approximate waves

Record name	Number of record points	Significant duration (sec)	Time (sec)		Percentage difference in time estimate (%)	
			Start	End	Start	End
Main	19890	10.83	19.58	30.41	-	-
A1	9945	10.98	19.58	30.56	0.00	0.476
A2	4972	11.02	19.58	30.60	0.00	0.608
A3	2486	11.12	19.60	30.72	0.102	1.002
A4	1244	11.52	19.68	31.20	0.510	2.580
A5	622	12.16	19.52	31.68	0.306	4.159

As can be seen from Table 3, the difference in the estimation of the starting time in all states is less than 3% and for the end time, until the A4 wave is less than 5%. The following two significant and uniform methods are used to analyze structures with multi degrees of freedom.

5 A new earthquake record in the duration of strong ground motion

In Fig. 7 the acceleration of the main earthquake and the records obtained by wavelet theory in five stages of using wavelet theory (A1 to A5) in a significant and uniform

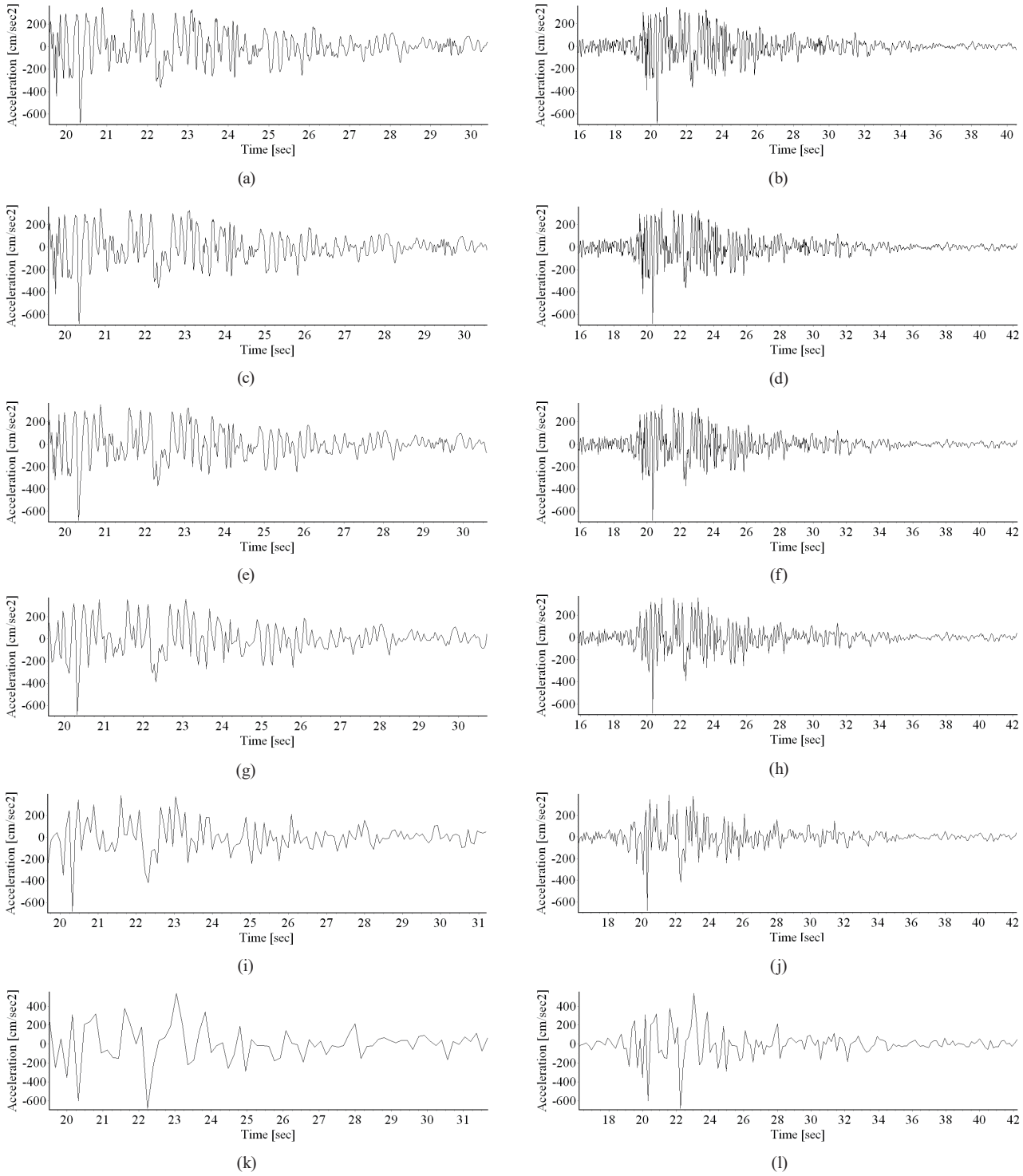

Fig. 7 Continued on next page

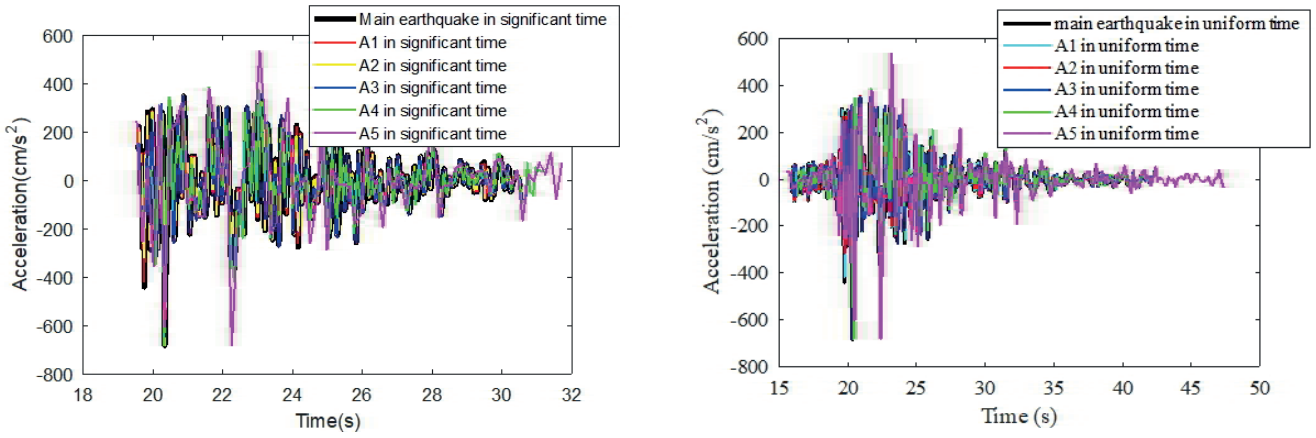

Fig. 7 a) Acceleration of the main earthquake in significant time, b) Acceleration of the main earthquake in uniform time, c) Wave A1 in significant time, d) Wave A1 in uniform time, e) Wave A2 in significant time, f) Wave A2 in uniform time, g) Wave A3 in significant time, h) Wave A3 in uniform time, i) Wave A4 in significant time, j) Wave A4 in uniform time, k) Wave A5 in significant time, l) Wave A5 in uniform time, m) Comparison of the acceleration curve of the main earthquake and waves A1 to A5 over an significant time, n) Comparison of the acceleration curve of the main earthquake and waves A1 to A5 over an uniform time

earthquake time are shown. The number of major earthquake records is 19890, which reduces by half the number at each stage of the use of the wavelet. The approximate wave points of A1 to A5 over the entire earthquake time (99.95 seconds) are 9945, 4972, 2486, 1244, and 622, respectively. The maximum acceleration of all waves has been scaled to the main peak ground acceleration (681.45 cm/sec2). To reduce computations, records are used that are significant and uniform over time. The number of records used for structural analysis using the significant time for the main earthquake and the approximate wave of A1 to A5 respectively was 2168, 1098, 551, 278, 144, and 76, and the number of records used for structural analysis using the significant time for the main earthquake and the approximate wave of A1 to A5 is 4930, 2638, 1320, 660, 325, and 199, respectively. In Table 4, the number of main earthquake points and each of the approximate waves and their percentage reduction is shown.

6 The results of solving two examples

6.1 Two-dimensional structures

In this part, the two-dimensional 7-story steel frame of Fig. 8 is analyzed and its dynamic response is obtained, and the results of a number of its nodes are compared with each other. The dynamic response of nodes 3, 6, 9, and 15 are calculated for the main acceleration and the records obtained after the application of the wavelet (waves A1 to A5) and the separation of the part that was important and uniform over time. The height of the frame floors is 3.2 meters, and the length of each opening is 6 meters. The density, the modulus of elasticity, and the yield stress of steel are 7800 kg/m^3, 2.04 × 10^{10} kg/m^2 and 3500 kg/m^2, respectively. The characteristics of the beams and columns are shown for each member.

In Fig. 9, the horizontal dynamic response of node 15 is plotted for the main earthquake acceleration.

Table 4 The number of different record points

Record name	Number of record points	Significant time		Uniform time	
		Number of record points	Percentage of points relative to the main record	Number of record points	Percentage of points relative to the main record
Main	19890	2168	10.90	4930	24.79
A1	9945	1098	5.52	2638	13.26
A2	4972	551	2.77	1320	6.64
A3	2486	278	1.40	660	3.32
A4	1244	144	0.72	325	1.63
A5	622	76	0.38	199	1.00

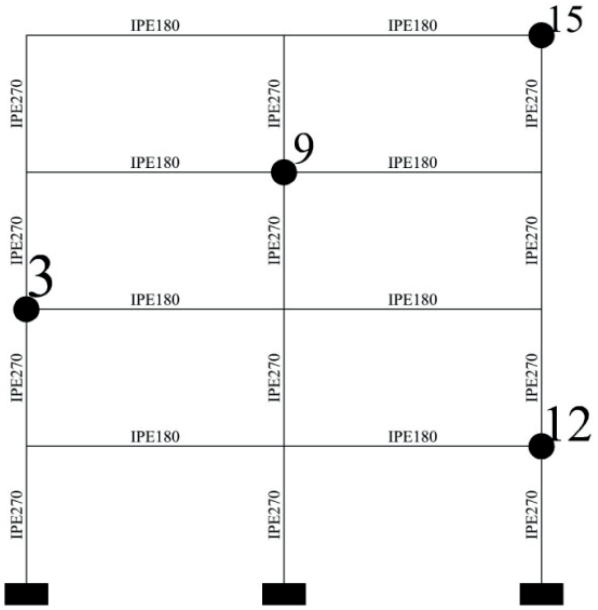

Fig. 8 Four story 2D frame

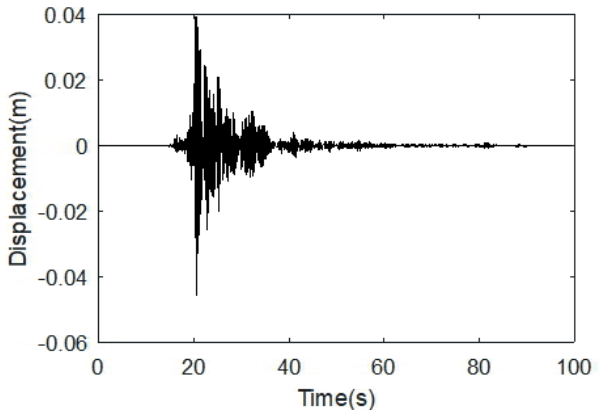

Fig. 9 Horizontal displacement of node 15 under the main earthquake

In Fig. 10, the horizontal displacement curve of node 15 is shown under the influence of the main earthquake and the waves A1 to A5. For this purpose, first using wavelet transform, approximate waves A1 to A5 are obtained, then using the concepts of significant time and uniform time, the strong part of each wave is extracted.

In Fig. 11, that part of the response curve of the structure under the main earthquake, which is significant time, is separated and shown with a thicker black line. It is clear from the figure that the response obtained using the A5 record is very different from the response obtained from other waves. But for A1 to A4 records, there is no significant difference.

In Fig. 12, that part of the response curve of the structure under the main earthquake, which is uniform time, is separated and shown with a thicker black line. It is clear from the figure that the response obtained using the A5 record is very different from the response obtained from other waves. But for A1 to A4 records, there is no significant difference.

Table 5 shows the maximum displacement of node 5 and its occurrence over a significant and uniform time. By examining the results, it can be seen that the use of the A4 wave with an error of less than 3% is the best alternative wave of the main earthquake wave. The number of points in this wave is 144 points, which is 138 times lower compared to the original wave of 19890 points. This reduction in the number of points reduces the computational volume.

Considering the response of node 15, it can be seen that if the A4 wave is used, the calculation is reduced by 98% and the error is close to 3%. Thus, in Table 6, the results of the displacement and the maximum rotation of several nodes of the structure for the A4 wave and its comparison with the main wave of the earthquake are shown.

6.2 Three-dimensional structure of five story

The three-dimensional structure shown in Fig. 13 is analyzed for the main earthquake, the main earthquake in a significant and uniform time, and the approximate waves A1 to A5 in a significant and uniform time. The steel frame has 5 floors and has Moment resisting connections and a rigid roof with a thickness of 25 cm. The height of all floors is 3 meters, and the length of all spans is 6 meters. Earthquake in the x direction affects the structure. The cross sections of the columns are IPE550 and the cross sections of the beams are IPE270. In this example, the density, the modulus of elasticity, and the yield stress of steel are 7800 kg/m^3, 2.04 ˜1010 kg/m^2 and 3500 kg/m^2, and the density, the modulus of elasticity, and the 28-day compressive strength of the concrete are 2400 kg m^3, 2.53 × 109 kg/m^2 and 28 MPa, respectively.

In Fig. 14, the horizontal dynamic response of node 42 along x is shown for the main earthquake.

In Fig. 15, the horizontal displacement curve of node 42 is shown for the main earthquake and the waves A1 to A5. For this purpose, first using wavelet transform, approximate waves A1 to A5 are obtained, then using the concepts of significant time and uniform time, the strong part of each wave is extracted.

In Fig. 16, that part of the response curve of the structure under the main earthquake, which is significant time, is separated and shown with a thicker black line. It is clear from the figure that the response obtained using the A5 record is very different from the response obtained from other waves. But for A1 to A4 records, there is no significant difference.

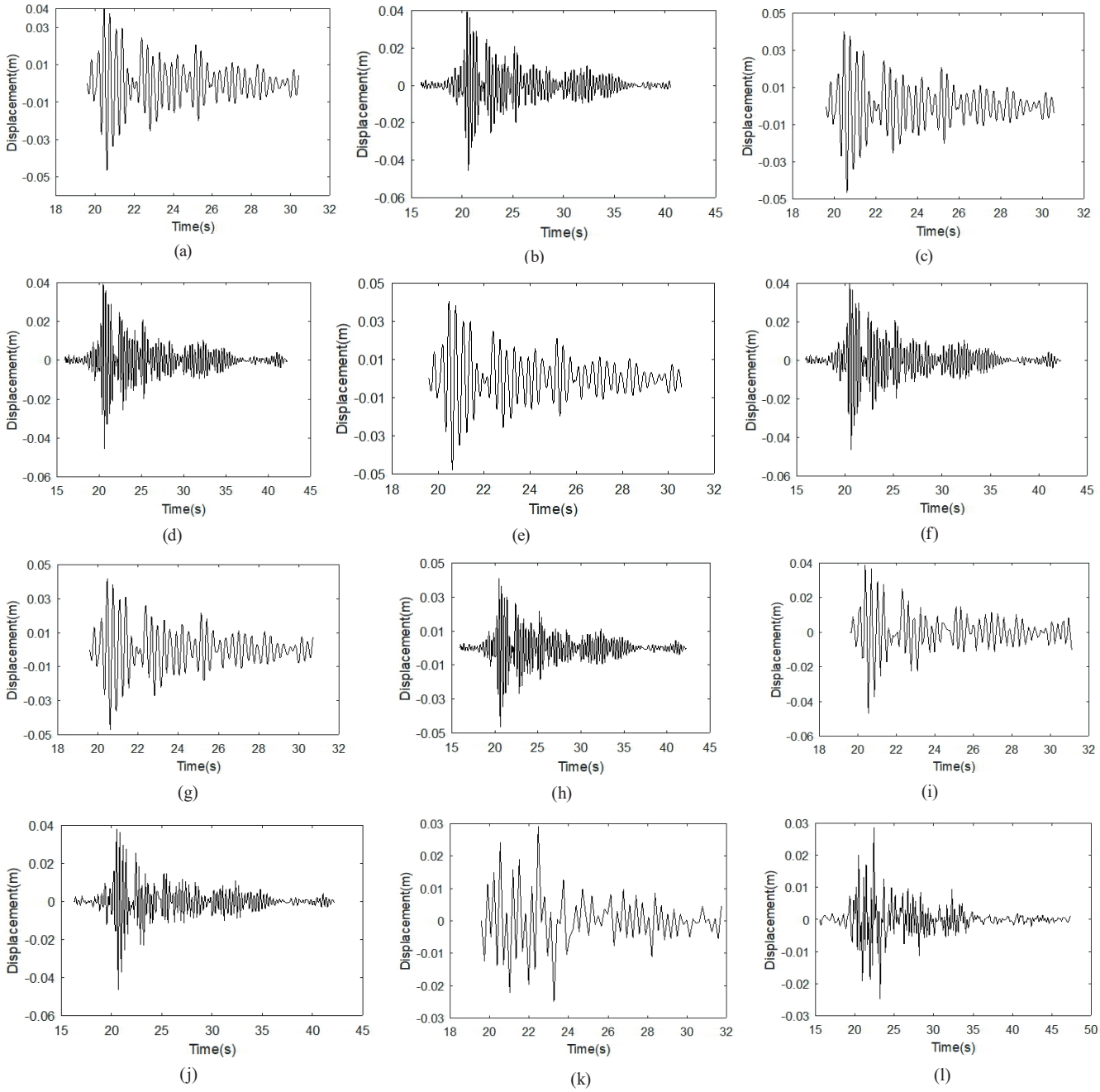

Fig. 10 a) Displacement of node 15 under the main earthquake in significant time, b) Displacement of node 15 under the main earthquake in uniform time, c) Displacement of node 15 under the A1 wave in significant time, d) Displacement of node 15 under the A1 wave in uniform time, e) Displacement of node 15 under the A2 wave in significant time, f) Displacement of node 15 under the A2 wave in uniform time, g) Displacement of node 15 under the A3 wave in significant time, h) Displacement of node 15 under the A3 wave in uniform time, i) Displacement of node 15 under the A4 wave in significant time, j) Displacement of node 15 under the A4 wave in uniform time, k) Displacement of node 15 under the A5 wave in significant time, l) Displacement of node 15 under the A5 wave in uniform time

In Fig. 17, that part of the response curve of the structure under the main earthquake, which is uniform time, is separated and shown with a thicker black line. It is clear from the figure that the response obtained using the A5 record is very different from the response obtained from other waves. But for A1 to A4 records, there is no significant difference.

Given that the A4 wave has reduced the computational volume by 98% and its error is close to 5%. Therefore, in Table 7, only the results at different points for the A4 wave and the main earthquake wave are examined.

As can be seen, using this method can reduce the computational volume to about 98%, while the error is always less than 8%.

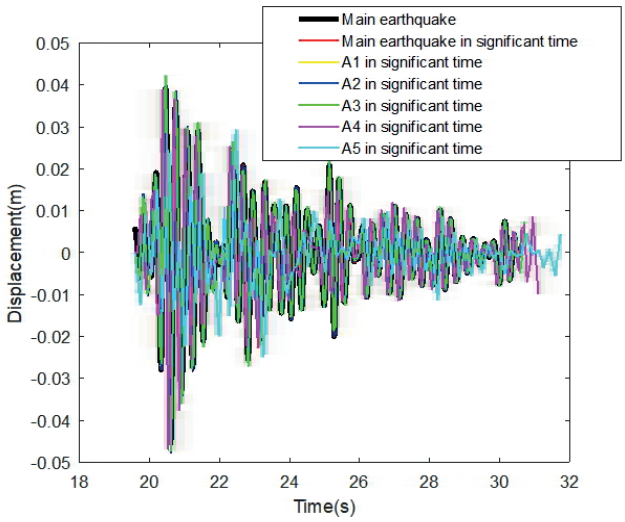

Fig. 11 Dynamic response of node 15 of the structure to the main earthquake and waves A1 to A5 over a significant time

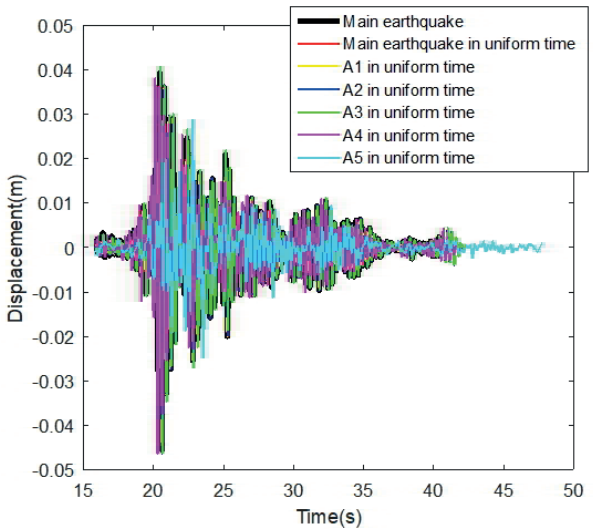

Fig. 12 Dynamic response of node 15 of the structure to the main wave and waves A1 to A5 over a uniform time

7 Conclusions

In this paper, for the first time, using the duration of strong ground motion and the wavelet filter, the dynamic analysis of the structure was carried out. In this regard, the earthquake wave was first corrected using the band-pass method. The modified wave was filtered using wavelet transforms to five stages. At each stage of the filter, two waves of approximations and details were obtained. Because the frequency content of the approximate wave is closer to the frequency content of the main earthquake wave, hence, for the next calculations, an approximation wave was used. At each stage, the approximate wave was scaled by the maximum acceleration of the main earthquake. After obtained of the approximate wave, the values of each of them were obtained in significant and uniform time. However, the earthquake wave points were reduced once by the wavelet transform and again by the concept of the duration of the strong ground motion. In fact, with wavelet transform, the time step of the analysis becomes larger, and with the duration of the strong ground motion, the duration of the analysis decreases. Then, two two-dimensional and three-dimensional structures against the earthquake were dynamically analyzed, and the dynamic response of some of their nodes was calculated in different directions. The results showed that:

1. In the case of significant time used, the A4 wave with an error of less than 8% is the best wave as a substitute for the main earthquake.
2. In the case of uniform time used, the wave A4 with an error of less than 6% is the best wave as the main earthquake substitute.
3. The A4 wave has reduced the volume of calculations by 138 times in significant time.
4. The A4 wave has reduced the volume of calculations by 62 times in uniform time.

Table 5 Horizontal displacement results of node 15 over a significant and uniform time period

Name Record	Significant Duration			Uniform Duration		
	Maximum displacement (cm)	Time of occurrence (sec)	Error calculating maximum displacement (%)	Maximum displacement (cm)	Time of occurrence (sec)	The maximum displacement calculation error (%)
Main	-4.548	20.61	-	-4.548	20.61	-
Main in significant or Uniform time	-4.643	20.61	2.08	-4.548	20.61	0.00
A1	-4.644	20.61	2.11	-4.536	20.62	0.21
A2	-4.776	20.62	5.01	-4.632	20.62	1.51
A3	-4.715	20.64	3.67	-4.622	20.64	1.33
A4	-4.681	20.64	2.92	-4.637	20.64	1.60
A5	-2.484	23.20	45.38	-2.470	23.20	37.45

Table 6 Displacement and Rotation of different structural points Example 1

Displacement (cm) or Rotation (rad)	The main wave at the time of the earthquake	Significant Duration		Uniform Duration	
		A4	Error percentage A4	A4	Error percentage A4
Displacement of node 9	3.53	3.66	3.68	3.63	2.83
Rotation of node 9	0.0033	0.0033	0.00	0.0033	0.00
Displacement of node 3	2.16	2.26	4.62	2.24	3.70
Rotation of node 3	0.0043	0.0044	2.32	0.0044	2.32
Displacement of node 12	0.74	0.79	6.76	0.78	5.40
Rotation of node 12	0.0036	0.0038	5.55	0.0037	2.77

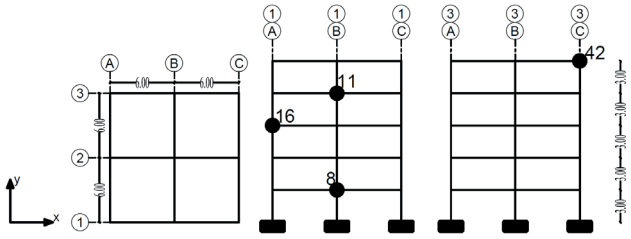

Fig. 13 3D frame

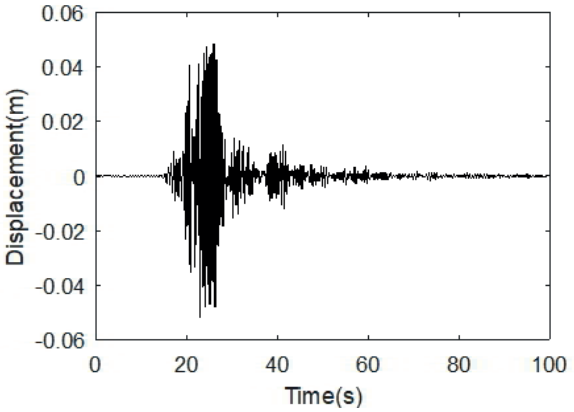

Fig. 14 Dynamic response of node 42 under the influence of the main earthquake during the total earthquake time

The advantage of the method presented in this paper compared to previous research is that this method simultaneously reduces the loading time and also corrects the earthquake time step. Therefore, this can lead to a reduction in the maximum computational cost in all dynamic analyzes, including earthquake loading. In all studies that have used wavelet transform to reduce earthquake record sampling, a reduction in computational costs of up to about 85% has been reported. But in this article, by combining the two concepts of the wavelet transform and the duration of strong ground motion, the cost of calculations can be reduced by more than 95%.

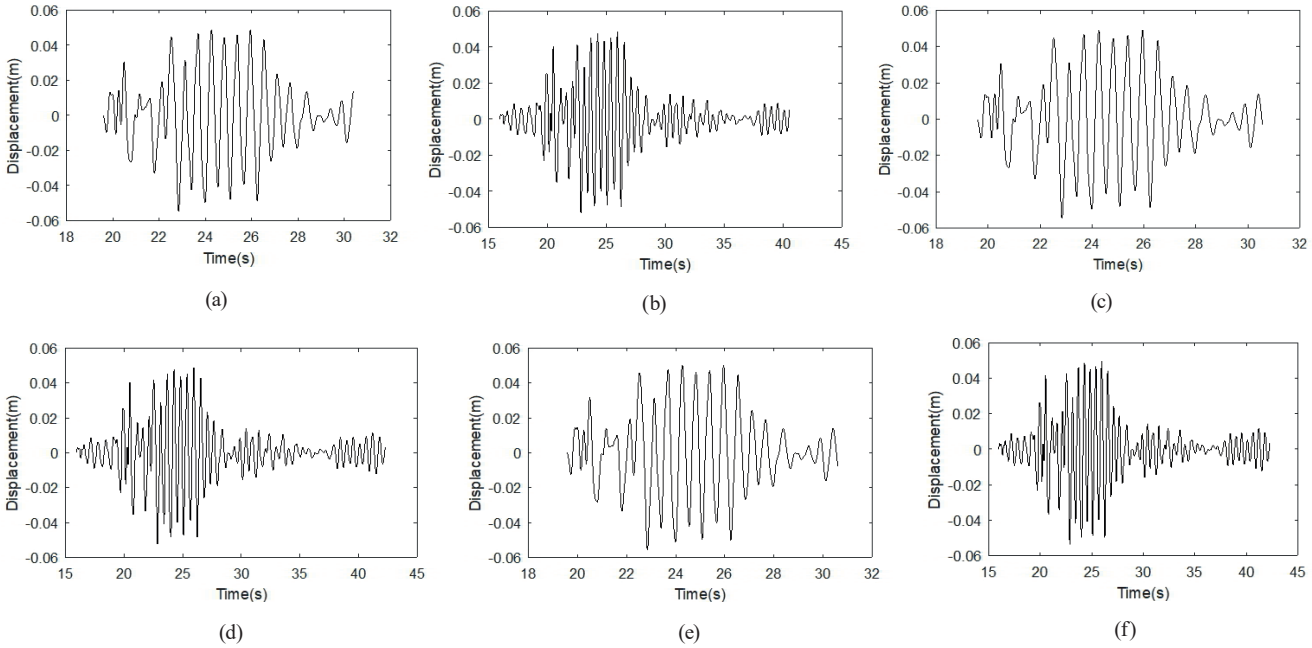

Fig. 15 Continued on next page

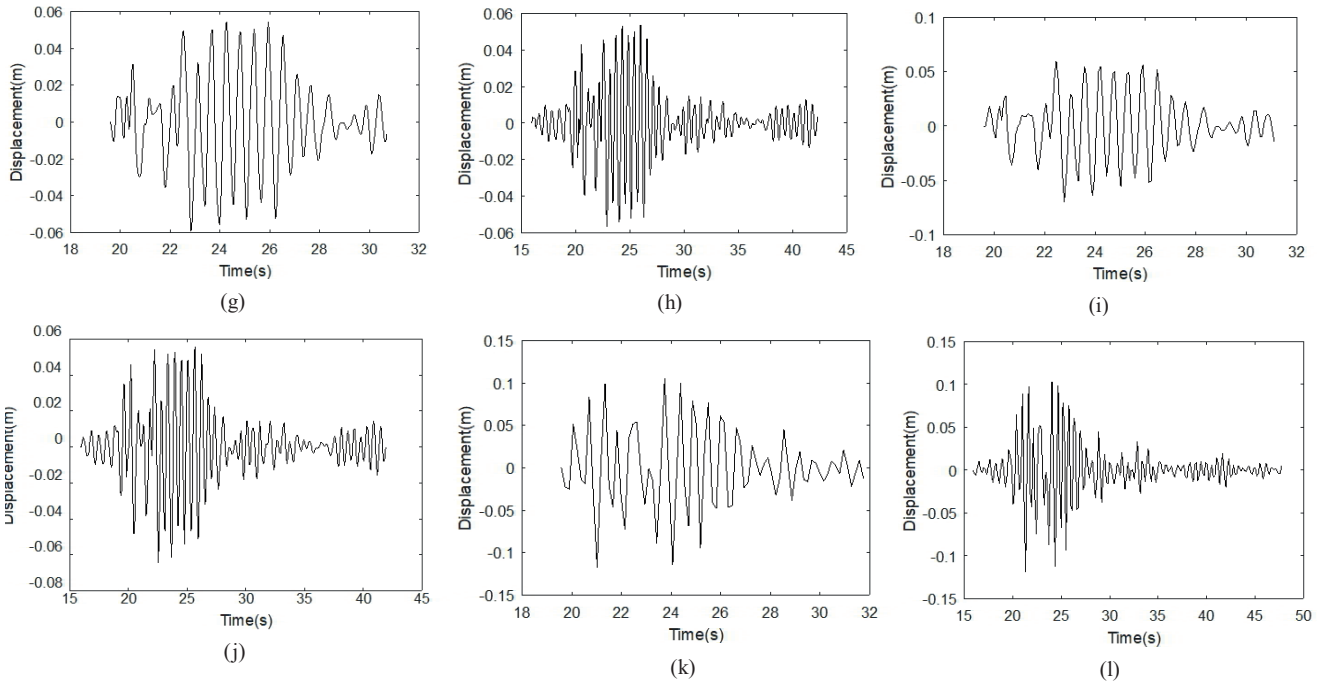

Fig. 15 a) Displacement of node 42 under the main earthquake in significant time, b) Displacement of node 42 under the main earthquake in uniform time, c)Displacement of node 42 under the A1 wave in significant time, d) Displacement of node 42 under the A1 wave in uniform time, e) Displacement of node 42 under the A2 wave in significant time, f) Displacement of node 42 under the A2 wave in uniform time, g) Displacement of node 42 under the A3 wave in significant time, h) Displacement of node 42 under the A3 wave in uniform time, i) Displacement of node 42 under the A4 wave in significant time, j) Displacement of node 42 under the A4 wave in uniform time, k) Displacement of node 42 under the A5 wave in significant time, l) Displacement of node 42 under the A5 wave in uniform time

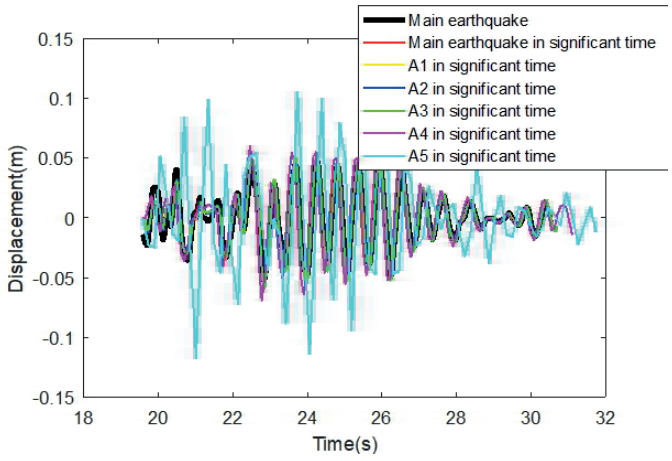

Fig. 16 Dynamic response of node 42 of the structure to the main wave and waves A1 to A5 over a significant time

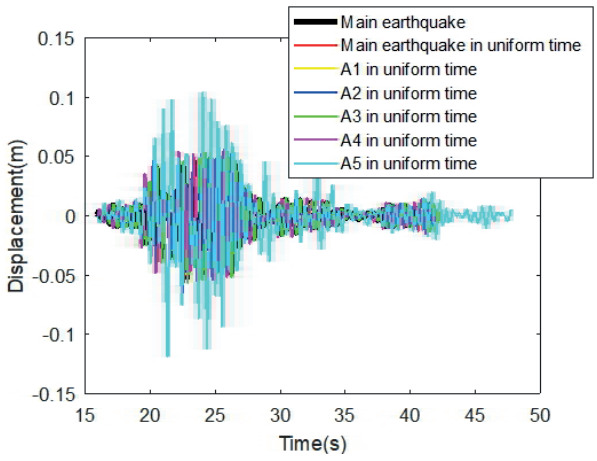

Fig. 17 Dynamic response of node 42 of the structure to the main wave and waves A1 to A5 over a uniform time

Table 7 Examination of the displacement and time of the various structural components

Displacement (cm) or Rotation (rad)	The main wave at the time of the earthquake	Significant Duration		Uniform Duration	
		A4	Error percentage A4	A4	Error percentage A4
Displacement of node 11	4.43	4.77	7.12	4.58	3.38
Rotation of node 11	0.23	0.24	4.34	0.23	0.00
Displacement of node 16	3.53	3.76	6.51	3.66	3.68
Rotation of node 16	0.12	0.12	0.00	0.12	0.00
Displacement of node 8	1.10	1.16	5.45	1.13	2.72
Rotation of node 8	0.09	0.09	0.00	0.09	0.00

References

[1] Katoh, S., Iio, Y., Katao, H., Sawada, M., Tomisaka, K., Miura, T., Yoneda, I. "The relationship between S-wave reflectors and deep low-frequency earthquakes in the northern Kinki district, south-western Japan", Earth, Planets and Space, 70, 149, 2018. https://doi.org/10.1186/s40623-018-0921-6

[2] Gupta, A. K. "Response spectrum method: in seismic analysis and design of structures", Blackwell Scientific Publications, 2017. ISBN: 9780849386282

[3] De Stefano, A., Ceravolo, R., Sabia, D. "Output only dynamic identification in time-frequency domain", In: Proceedings of the 2001 American Control Conference, Arlington, VA, USA, 2001, pp. 447–452. https://doi.org/10.1109/ACC.2001.945585

[4] Marasco, S., Cimellaro, G. P. "A new energy-based ground motion selection and modification method limiting the dynamic response dispersion and preserving the median demand", Bulletin of Earthquake Engineering, 16, pp. 596–618, 2018. https://doi.org/10.1007/s10518-017-0232-5

[5] Vassiliou, M. F., Makris, N. "Estimating time scales and length scales in pulselike earthquake acceleration records with wavelet analysis", Bulletin of the Seismological Society of America, 101(2), pp. 596–618, 2011. https://doi.org/10.1785/0120090387

[6] Bolt, B. A. "Duration of strong ground motion", In: Proceedings of the 5th World Conference on Earthquake Engineering, Rome, Italy, 1973, pp. 1304–1313.

[7] Trifunac, M. D., Brady, A. G. "A study on the duration of strong earthquake ground motion", Bulletin of the Seismological Society of America, 65(3), pp. 581–626, 1975. https://doi.org/10.1785/BSSA0650030581

[8] Trifunac, M. D. "A method for synthesizing realistic strong ground motion", Bulletin of the Seismological Society of America, 61(6), pp. 1739–1753, 1971. https://doi.org/10.1785/BSSA0610061739

[9] Walter, G. G., Shen, X. "Wavelets and other orthogonal systems", CRC press, 2000. ISBN: 9781315273716 https://doi.org/10.1201/9781315273716

[10] Salajegheh, E., Heidari, A. "Dynamic analysis of structures against earthquake by combined wavelet transform and fast Fourier transform", Asian Journal of Civil Engineering, 3(3–4), pp. 75–87, 2002.

[11] Salajegheh, E., Heidari, A. "Time history dynamic analysis of structures using filter banks and wavelet transforms", Computers & structures, 83(1), pp. 53–68, 2005. https://doi.org/10.1016/j.compstruc.2004.08.008

[12] Salajegheh, E., Heidari, A. "Optimum design of structures against earthquake by adaptive genetic algorithm using wavelet networks", Structural and Multidisciplinary Optimization, 28, pp. 277–285, 2004. https://doi.org/10.1007/S00158-004-0422-Z

[13] Heidari, A., Majidi, N. "Earthquake acceleration analysis using wavelet method", Earthquake Engineering and Engineering Vibration, 20, pp. 113–126, 2021. https://doi.org/10.1007/s11803-021-2009-8

[14] Majidi, N., Heidari, A. "Investigation of the natural frequency of the structure and earthquake frequencies in the frequency domain using a discrete wavelet", Sharif Journal of Science and Technology, 36(2), pp. 105–113, 2019. (in Persian) https://doi.org/10.24200/j30.2019.52464.2472

[15] Heidari, A., Salajegheh, E. "Time history analysis of structures for earthquake loading by wavelet networks", Asian Journal of Civil Engineering, 7(2), pp. 155–168, 2006.

[16] Heidari, A., Salajegheh, E. "Wavelet Analysis for Processing of Earthquake Records", Asian Journal of Civil Engineering, 9(5), pp. 513–524, 2009.

[17] Heidari, A. "Optimum design of structures for earthquake induced loading by genetic algorithm using wavelet transform", Advances in Applied Mathematics & Mechanics, 2, pp. 107–117, 2010. https://doi.org/10.4208/aamm.09-m0932

[18] Heidari, A., Raeisi, J., Pahlavan Sadegh, S. "Dynamic analysis of shear building structure using wavelet transform", Journal of Numerical Methods in Civil Engineering, 2(4), pp. 20–26, 2018. https://doi.org/10.29252/nmce.2.4.20

[19] Heidari, A., Pahlavan Sadegh, S., Raeisi, J. "Investigating the Effect of Soil Type on Non-linear Response Spectrum Using Wavelet Theory", International Journal of Civil Engineering, 17, pp. 1909–1918, 2019. https://doi.org/10.1007/s40999-019-00394-6

[20] Rad, M. M., Habashneh, M., Lógó, J. "Elasto-Plastic limit analysis of reliability based geometrically nonlinear bi-directional evolutionary topology optimization", Structures, 34, pp. 1720–1733, 2021.

[21] Rad, M. M., Ibrahim, S. K. "Optimal Plastic Analysis and Design of Pile Foundations Under Reliable Conditions", Periodica Polytechnica Civil Engineering, 65(3), pp. 761–767, 2021. https://doi.org/10.3311/PPci.17402

[22] Kamgar, R., Majidi, N., Heidari, A. "Wavelet-based decomposition of ground acceleration for efficient calculation of seismic response in elastoplastic structures", Periodica Polytechnica Civil Engineering, 65(2), pp. 409–424, 2021. https://doi.org/10.3311/PPci.14475

[23] Kamgar, R., Dadkhah, M., Naderpour, H. "Seismic response evaluation of structures using discrete wavelet transform through linear analysis", Structures, 29, pp. 863–882, 2021. https://doi.org/10.1016/j.istruc.2020.11.012

[24] Dadkhah, M., Kamgar, R., Heidarzadeh, H. "Reducing the cost of calculations for incremental dynamic analysis of building structures using the discrete wavelet transform", Journal of Earthquake Engineering, 26(7), pp. 3317–3342, 2020. https://doi.org/10.1080/13632469.2020.1798830

[25] Kamgar, R., Tavakoli, R., Rahgozar, P., Jankowski, R. "Application of discrete wavelet transform in seismic nonlinear analysis of soil–structure interaction problems", Earthquake Spectra, 37(3), pp. 1980–2012, 2021. https://doi.org/10.1177/8755293020988027

[26] Javdanian, H., Heidari, A., Raeisi, J. "Seismic ground response under wavelet-based decomposed earthquake records", Soil Dynamics and Earthquake Engineering, 149, 106865, 2021. https://doi.org/10.1016/J.SOILDYN.2021.106865

[27] Majidi, N., Tajmir Riahi, H., Zandi, M. "Reducing computational efforts in linear and nonlinear analysis of peridynamic models under impact loads", Amirkabir Journal of Civil & Environmental Engineering, 2022. (in Persian)
https://doi.org/10.22060/CEEJ.2022.20075.7337

[28] Shabankhah, S., Heidari, A., Kamgar, R. "Optimum level of discrete wavelet decomposition for dynamic analysis of hydraulic structures", International Journal of Optimization in Civil Engineering, 11(4), pp. 631–646, 2021.

[29] Majidi, N., Heidari, A., Alireza, F., Heidarzadeh, H. "Estimation of earthquake frequency content and its effect on dynamic analysis using continuous and discrete wavelet transform", Scientia Iranica, in press. (Accepted for publication: January 10)
https://doi.org/10.24200/SCI.2022.54226.3662

[30] Kankanamge, Y., Hu, Y., Shao, X. "Application of wavelet transform in structural health monitoring", Earthquake Engineering and Engineering Vibration, 19, pp. 515–532, 2020.
https://doi.org/10.1007/s11803-020-0576-8

[31] Harikrishnan, M. G., Gupta, V. K. "Scaling of residual displacements in terms of elastic and inelastic spectral displacements for existing SDOF systems", Earthquake Engineering and Engineering Vibration, 19, pp. 71–85, 2020.
https://doi.org/10.1007/s11803-020-0548-z

[32] Nagarajaiah, S., Basu, B. "Output only modal identification and structural damage detection using time frequency & wavelet techniques", Earthquake Engineering and Engineering Vibration, 8, pp. 583–605, 2009.
https://doi.org/10.1007/s11803-009-9120-6

[33] Ding, Y., Li, A. "Structural health monitoring of long-span suspension bridges using wavelet packet analysis", Earthquake Engineering and Engineering Vibration, 6, pp. 289–294, 2007.
https://doi.org/10.1007/s11803-007-0746-y

[34] Bose, N. K. "Wavelets and Filter Banks", In: Applied Multidimensional Systems Theory, Springer, 2017, pp. 161–188. ISBN: 978-3-319-46824-2
https://doi.org/10.1007/978-3-319-46825-9_6

[35] Mallat, S. G. "A theory for multiresolution signal decomposition: the wavelet representation", IEEE Transactions on Pattern Analysis and Machine Intelligence, 11(7), pp. 674–693, 1989.
https://doi.org/10.1109/34.192463

[36] Sheng, Y. "Wavelet transform", In: The Transforms and Applications Handbook Series, CRC Press, 1996, pp. 747–827. ISBN: 9781420066524

[37] Hamidian, D., Salajegheh, E., Salajegheh, J. "Irregular Continuum Structures Damage Detection based on Wavelet Transform and Neural Network", KSCE Journal of Civil Engineering, 22, pp. 4345–4352, 2018.
https://doi.org/10.1007/s12205-018-1470-z

[38] Housner, G. W. "Intensity of earthquake ground shaking near the causative fault", In: Proceedings of the Third World Conference on Earthquake Engineering, Auckland, Wellington, New Zealand, 1965, pp. 94–115.

[39] Reinoso, E., Ordaz, M. "Duration of strong ground motion during Mexican earthquakes in terms of magnitude, distance to the rupture area and dominant site period", Earthquake Engineering and Structural Dynamics, 30(5), pp. 653–673, 2001.
https://doi.org/10.1002/eqe.28

[40] Wong, H. L., Trifunac, M. D. "Generation of artificial strong motion accelerograms", Earthquake Engineering and Structural Dynamics, 7(6), pp. 509–527, 1979.
https://doi.org/10.1002/eqe.4290070602

[41] Housner, G. "Measures of severity of earthquake ground shaking", In: Proceedings of the US National Conference on Earthquake Engineering, Ann Arbor, MI, USA, 1975, pp. 25–33.

[42] Bommer, J. J., Martínez-Pereira, A. "The effective duration of earthquake strong motion", Journal of Earthquake Engineering, 3(2), pp. 127–172, 1999.
https://doi.org/10.1080/13632469909350343

[43] Kramer, S. L. "Geotechnical Earthquake Engineering", Prentice-Hall, 1996. ISBN: 0-13-374943-6

[44] Heidari, A., Majidi, N. "Investigation of the natural frequency of the structure and earthquake frequencies in the frequency domain using a discrete wavelet", Sharif Journal of Civil Engineering, 36(2), pp. 105–113, 2019. (in Persian)
https://doi.org/10.24200/j30.2019.52464.2472

[45] Kayani, K., Majidi, N., Heidari, A. "Investigating the Application of Wavelet Transform and Fourier Spectrum in the Frequency Content of the Sarpolzahab Earthquake Wave", presented at: 2nd International Congress on Science & Engineering, Hamburg, Germany, March, 12, 2019.

[46] Kayani, K., Majidi, N., Heidari, A. "Investigation of the effect of earthquake record reduction on structure response in frequency domain using wavelet transform", presented at: 2nd International Congress on Science & Engineering, Hamburg, Germany, March, 12, 2019.